GLOBAL PATTERNS AND INTER-ANNUAL VARIABILITY IN CARBON DIOXIDE DEPOSITION ON MARS: INFRARED OBSERVATIONS FROM THE MARS CLIMATE SOUNDER. P. O. Hayne[1], S. Piqueux[1], A. Kleinböhl[1], D. M. Kass[1], D. J. McCleese[1] [1]NASA – Jet Propulsion Laboratory, California Institute of Technology (Paul.O.Hayne@jpl.nasa.gov)

Introduction: In the present climate system of Mars, the exchange of carbon dioxide between the surface and atmosphere plays a central role through its regulation of global atmospheric pressures and its influence on general circulation [1,2]. Carbon dioxide deposition has also been recognized as a fundamental process in the past climates of Mars [3,4,5]. Cloud formation and CO_2 snowfall have been observed at both winter poles [6,7], measurably altering the planetary heat balance [8,9,10]. Understanding this present-day cycle of CO_2 may elucidate the collapse of a thicker atmosphere within the last few million years, a remnant of which may now be trapped in the southern polar layered deposits [11,12].

Here, we report a study of CO_2 deposition at the winter poles using infrared data spanning more than five Mars Years (MY). We investigated the spatial distribution and time-variability in CO_2 snowfalls and frosts in both hemispheres. This study reveals new aspects of volatile exchange in the martian polar regions, with links to climatic processes operating on diurnal, seasonal, and inter-annual timescales.

Data and Methods: The Mars Reconnaissance Orbiter's Mars Climate Sounder (MCS) investigation [13] utilizes a multi-band infrared and solar radiometer to probe the atmosphere and surface of Mars in nine spectral channels. We utilized retrieved atmospheric profiles [14] of temperature, pressure, and aerosol opacity (dust, H_2O, CO_2), as well as surface brightness temperatures indicative of the presence and physical state of condensed volatiles. Previous work has shown that brightness temperatures at 22 and 32 μm below the local CO_2 frost point are caused primarily by CO_2 clouds and snowfalls, which contribute significant material to the seasonal ice caps [15]. In the present study, we identified regions of active or recent snowfalls based on an empirical criterion: $T_{CO2} - T_{32\mu} > 10$ K and $T_{12\mu} - T_{32\mu} > 5$ K, where T_{CO2} is the CO_2 frost point (calculated using retrieved surface pressures) and T_{λ} is the retrieved surface brightness temperature at wavelength λ. Previous work [15,16] has shown that these "cold spots" fade on approximately diurnal timescales unless replenished by snowfall. We also performed a series of targeted observation campaigns with MCS to detect and monitor polar clouds [17]. Finally, we built a climate record with the MCS data to identify variability across six Mars years: MY 28 – 33.

Results: Consistent patterns of polar snowfalls and correspondingly low brightness temperatures emerge from the multi-year MCS data (Fig. 1). In the northern hemisphere, fine-grained deposits (low $T_{32\mu}$) show a longitudinal asymmetry corresponding to a predominant mode-3 and mode-2 wave pattern, consistent with enhanced snowfall in longitudes ~0–120°E and 180–270°E, in latitudes ~65–75°N. Multiple smaller ~100-km features also persist, notably one near 165°E,

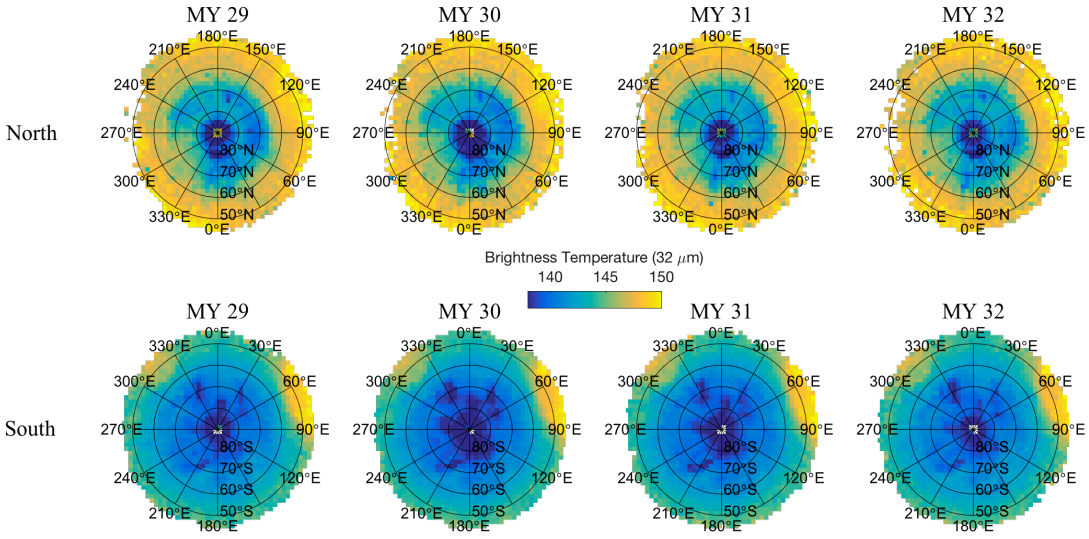

Figure 1: Polar stereographic maps of mean annual brightness temperature measured by MCS at 32 μm. Here, the data averaged include only those measurements where CO_2 frost was detected on the surface.

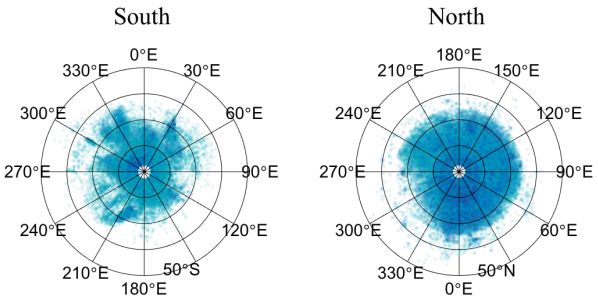

Figure 2: Polar stereographic maps of CO_2 snow detections from MCS (see text). Data are from all available years, MY 28 – 33. Darker shades indicate larger deviations from the local CO_2 frost point.

72°N. In the southern hemisphere, these smaller-scale features dominate, and are typically associated with ~100-km scale topography.

These features are even more pronounced when all of the snowfall detections over MY 28-33 are plotted together (Fig. 2). In this case, it is clear that snowfalls are much more pervasive in the northern hemisphere, with nearly complete coverage down to ~75°N latitude. Southern hemisphere deposition is much more heterogeneous. These patterns are expressed in the mean 32-μm brightness temperature (Fig. 1) of the seasonal ice caps, where the northern cap shows much lower emissivity than its southern counterpart, especially at latitudes >80°. Targeted limb observations (not shown) also reveal hemispheric and longitudinal differences in cloud composition (more water ice in northern winter) and prevalence (more CO_2 snow clouds in the north). Significant inter-annual variability is observed, particularly in the "snowiest" regions of both hemispheres.

Carbon dioxide frost occurs at nearly all latitudes on Mars, not just in the polar regions [18]. Figure 3 shows this and other unexpected CO_2 deposition features, including an early spring burst of activity in latitudes ~60–75°S, as well as throughout the summer at the south polar residual cap (SPRC, lat > 87°S).

Discussion: Seasonal CO_2 deposition in Mars' polar regions shows remarkable repeatability from one year to the next (Fig. 1). The same wave-like pattern is established in the north, whereas topography (orography) dominates precipitation in the south. However, significant variability in the MCS brightness temperatures from year to year indicates changes in the mode (and perhaps magnitude) of deposition. In particular, MY 30 (2009–2011) was a particularly cold year in both hemispheres overall, although isolated regions showed the opposite behavior. This could indicate colder atmospheric temperatures and/or greater availability of ice condenation nuclei to promote CO_2 precipitation. We do not observe any secular change in Mars' polar climate over the four-Mars-year period MY 29 – 32. Further observations by MCS will strengthen the constraints on models and provide a climate record for the polar regions that can be a basis for extrapolation of models to past climatic regimes.

References: [1] Leighton, R. B., & Murray, B. C. (1966), *Science*, *153*(3732), 136-144. [2] Pollack, J. B., et al. (1990), *J. Geophys. Res.*, *95*(B2), 1447-1473. [3] Sagan, C., et al. (1973), *Science*, *181*(4104), 1045-1049. [4] Ward, W. R. (1974). *J. Geophys. Res.*, *79*(24), 3375-3386. [5] Forget, F., et al. (2013), *Icarus*, *222*(1), 81-99. [6] Neumann, G. A., et al. (2003), *J. Geophys. Res.*, *108*(E4). [7] Colaprete, A., & Toon, O. B. (2002), *J. Geophys. Res.*, *107*(E7). [8] Paige, D. A., & Ingersoll, A. P. (1985), *Science 228*(4704):1160-8. [9] Forget, F., et al. (1995), *J. Geophys. Res.*, *100*(E10), 21219-21234. [10] Hayne, P. O., et al. (2012), *J. Geophys. Res.*, *117*(E8). [11] Phillips, R. J., et al. (2011), *Science*, *332*(6031), 838-841. [12] Bierson, C. J., et al. (2016), *Geophys. Res. Lett.*, *43*(9), 4172-4179. [13] McCleese, D. J., et. al. (2007), *J. Geophys. Res.*, *112*(E5). [14] Kleinböhl, A., et al. (2009), *J. Geophys. Res.*, *114*(E10). [15] Hayne, P. O., et al. (2014), *Icarus*, *231*, 122-130. [16] Cornwall, C., & Titus, T. N. (2010), *J. Geophys. Res.*, *115*(E6). [17] Hayne, P. O., et al. (2015), *AGU Fall Meeting*, #P22A-02. [18] Piqueux, S., et al. (2016), *J. Geophys. Res.*, *121*(7), 1174-1189.

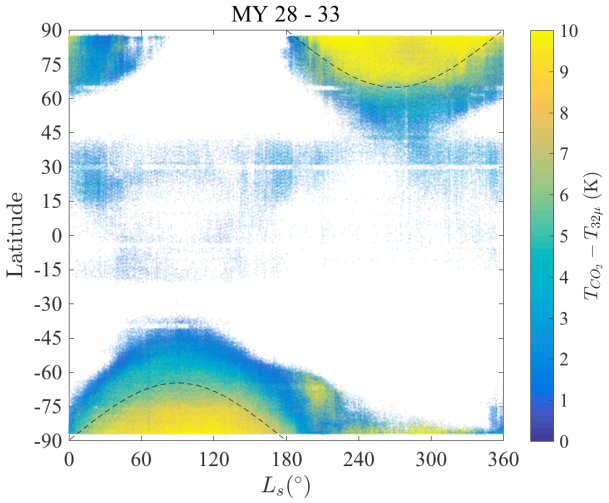

Figure 3: Detections of CO_2 frost on Mars' surface from MCS data. Colors indicate deviation from the local frost point, where brighter colors indicate snowfall and/or fine-grained frost.

Acknowledgement: Part of this work was performed at the Jet Propulsion Laboratory, California Institute of Technology, under contract with the National Aeronautics and Space Administration.